

Electrooptically Tunable Folded Arrayed Waveguide Grating Multiplexer

Kevin D. Le, Nikolai Stelmakh, *Senior Member, IEEE*, Michael Vasilyev, *Member, IEEE*, and J. C. Chiao, *Member, IEEE*

Abstract—Channel tunability of 10 GHz has been demonstrated in a 40-channel 50-GHz-spaced folded silica-on-silicon arrayed waveguide grating (AWG) multiplexer using quadratic nonlinearity in phosphorous-doped glass and a specially shaped electrode. Such AWG can be stabilized and tuned around ITU grid without power-consuming thermoelectric coolers.

Index Terms—Integrated optics, multiplexers, optical couplers, optical switches, planar waveguides.

LOW INTRINSIC losses, ease of fabrication, and natural mode match with optical fibers have made the silica-on-silicon planar lightwave circuits (PLCs) one of the dominant technologies for passive optical components, such as couplers, variable attenuators, interleavers, arrayed waveguide grating (AWG) multiplexers–demultiplexers, dynamic spectral equalizers, and even optical cross-connects [1]–[3]. One of the drawbacks of this silica technology is the temperature dependence of the PLC devices, owing to their interferometric nature. This requires the use of thermoelectric coolers that consume significant electric power and often require external heat-dissipating infrastructure. The same applies to thermo-optical tuning of these devices. Low-power-consuming methods of stabilizing and tuning the PLCs, needed, for example, for precise positioning of AWGs on the ITU grid, are, therefore, of great interest.

In this letter, we use quadratic electrooptic (EO) effect in phosphorus-doped silica to demonstrate the tunability of the AWG. In our experiment, we utilize folded design of AWG [4], [5]. Such design considerably improves the nonuniformity of insertion losses and the size of the chip while increasing the free spectral range. Due to a double pass of light through EO-controlled waveguide grating area, the tuning efficiency is doubled. In addition, the small size of the folded grating makes its fabrication compatible with conventional silicon foundry and standard photolithography equipment.

The folded 40-channel 50-GHz-channel-spacing AWG multiplexer–demultiplexer chip was fabricated by high-pressure oxidation process and plasma-enhanced chemical vapor deposition process in P-5000 machine. The refractive index contrast of AWG waveguides was approximately 0.8%. To fit 2×2 cm stepper photolithography field, typically used at complimentary metal–oxide–semiconductor foundries, the design of 50-GHz

AWG has been modified: Grating areas with strong coupling effects between waveguides have been replaced by an extended length of slab area between coupler and grating. Such 50-GHz 40-channel AWG chip with a high-reflectivity folding mirror has demonstrated 2.4-dB fiber-to-fiber insertion loss, total insertion-loss uniformity of 0.5 dB across all 40 channels, polarization-dependent loss of less than 0.35 dB, and -45 dB value of background crosstalk without any postfabrication trimming [4]. In the present study, the mirror side of the AWG chip is not coated, but is simply polished with diamond laps after high-precision dicing.

The P_2O_5 - and B_2O_3 -doped silica glasses, widely used in planar waveguide fabrication, have low third-order refractive index susceptibility [6], [7]. The nonlinearity of optical waveguides fabricated from such glasses is close to that of pure fused silica, i.e., $\chi_{1111}^{(3)} = 2.3 \times 10^{-22} \text{ (m/V)}^2$ [8]. The typical values of electrical breakdown in boro- and phospho-silicate glass are about $600 \text{ V}/\mu\text{m}$ [9]. Therefore, the order of magnitude of maximum Kerr index variation that can be achieved in such a glass system is $\Delta n \sim 10^{-4}$. Even though such index variations are small, they are able to create notable phase variations in PLC devices with significant lengths such as, for example, AWGs, interleavers, and Mach–Zehnder interferometers. The EO phase increment between the waveguides translates into a frequency shift of the transfer function.

The EO tuning efficiency can be significantly enhanced by a design of the electrode that maximizes the induced interwaveguide phase increment. Let us consider two cases: Case 1 of a simplest electrode and Case 2 of the optimum electrode. *Case 1*: The two neighboring waveguides of AWG have geometrical length difference equal to D . Therefore, if both waveguides are covered by a common EO electrode, the induced phase difference is equal to $k_0 D \Delta n$, where k_0 –propagation wave number and Δn –induced refractive index variation under applied electrical field. *Case 2*: In addition to the geometrical length difference between the adjacent waveguides, we further reduce the length of the shorter (closer to the center O of the AWG in Fig. 1) waveguide’s electrode by Δl_e . In this case, the phase difference between our two waveguides is $k_0 (D + \Delta l_e) \Delta n = k_0 D (1 + \xi) \Delta n$, where $\xi = \Delta l_e / D$ is the enhancement factor of the electrode. This enhancement factor can also be made negative by reversing the direction of electrode length difference increment. In the case of AWG with quasi-circularly bended waveguides, the maximum enhancement factor $\xi = R_{\max} / (R_{\max} - R_{\min})$ is determined by the geometry of electrode. Such design of electrode maximizes the tuning for a given voltage and is shown as an insert in Fig. 1. To form the EO electrode, a 300-nm-thick

Manuscript received May 25, 2004; revised July 28, 2004.

The authors are with the Department of Electrical Engineering, University of Texas at Arlington, Arlington, TX 76019-0016 USA (e-mail: nikolais@uta.edu).

Digital Object Identifier 10.1109/LPT.2004.838303

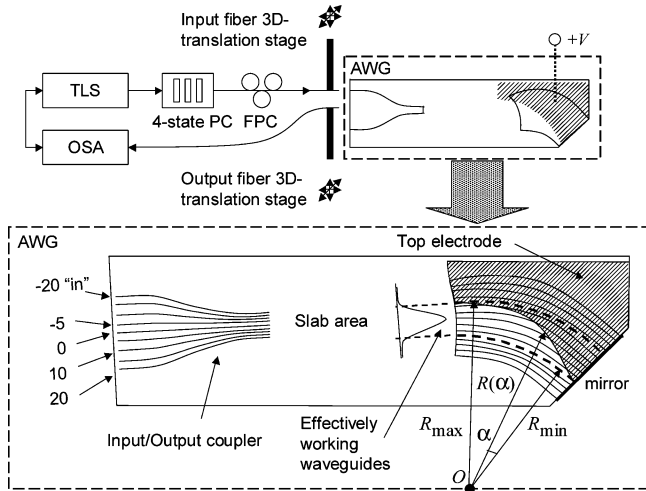


Fig. 1. Experimental setup and layout of the electrode for AWG tuning. OSA: Optical spectrum analyzer.

layer of gold is deposited on top of the grating waveguides through a contact mask fabricated specifically for the present design of AWG. The silicon substrate with electrical resistivity of $10 \Omega \cdot \text{cm}$ plays a role of the bottom electrode and is connected to the ground with the help of electroconductive glue. These two electrodes are spaced by $32 \mu\text{m}$ of glass and create a transversal electric field in AWG waveguides. A dc voltage in the range between 0 and 8 kV is applied to the top electrode by a wire protected by a glass tube. The whole system is sealed by a conventional epoxy.

We have measured the polarization-dependent transmission spectra of AWG using a $1.55\text{-}\mu\text{m}$ tunable laser source (TLS) and optical spectrum analyzer. Emission from TLS was delivered to the “input” waveguide of AWG through a four-state polarization controller (PC) and a manual fiber PC (FPC), as shown in Fig. 1. At the initial calibration step, the input fiber is moved up and light from the fiber is directed to a power meter through a polarizer. By adjustment of FPC, a minimum of power is obtained. Switching the four-state PC to the orthogonal polarization results in maximum transmission through the polarizer. The extinction ratio obtained in this calibration process is around 1000. Then, the input fiber is lowered, and both input and output fibers are aligned to the AWG chip, using x , y , z , and λ iterative optimizations. Assuming no change in the polarization state during the process of fiber lowering, the described procedure allows us to launch either the transverse electric (TE) [horizontal, or parallel to the AWG surface plane] or transverse magnetic (TM) [vertical] polarizations into the AWG. After calibration, the two orthogonal states of the four-state PC correspond to TE and TM modes. The output signal is collected from several output channels of AWG indexed -5 , 0 , $+10$, $+20$ (see Fig. 1). For simplicity of the electrode fabrication, no coating was deposited onto the AWG mirror. All the transmission spectra are obtained with a bare mirror having reflection $R \sim 3.4\%$ or -14.7 dB at glass–air interface. The optical power in the input fiber is $+1.5 \text{ dBm}$. The difference between the measured spectra and a reference level of $(1.5 - 14.7) \text{ dBm} = -13.2 \text{ dBm}$ corresponds to transmission performance of the packaged device with dielectrically coated mirror.

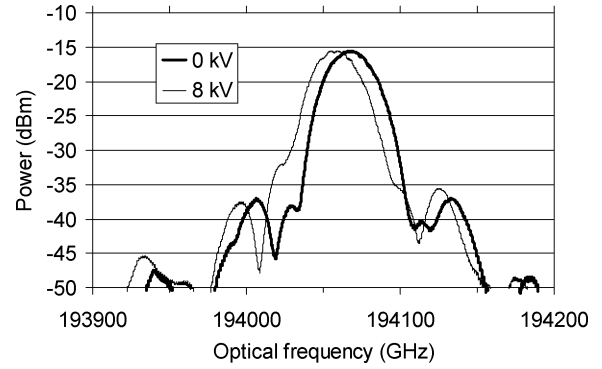


Fig. 2. EO shift of the transmission spectrum of AWG at Channel 0 (1545.85 nm) and vertical input polarization.

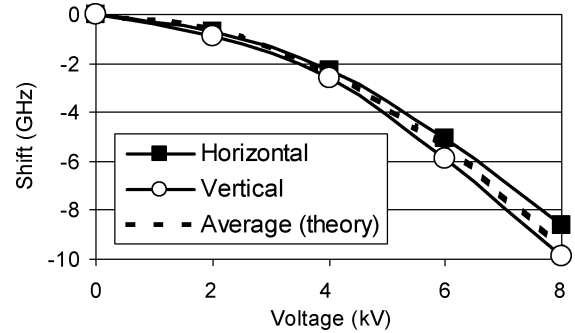


Fig. 3. Frequency shift for Channel 0 (1545.85 nm) as a function of applied voltage for both TE (horizontally polarized) and TM (vertically polarized) input signals. The dashed line shows the theoretical dependence calculated for fused silica in assumption of complete polarization averaging.

Fig. 2 shows the transmission spectra obtained from Channel 0 of AWG for two applied voltages, 0 and 8 kV. Vertical orientation of the input optical field is used in these measurements. One can see no significant change in the shape of spectral curve and in the value of the crosstalk under conditions of 8 kV of applied voltage. Fig. 3 summarizes the dependence of the spectral shift on the applied voltage for both vertical and horizontal input polarizations. Fig. 4 shows the good uniformity of tuning phenomena across the different channels of AWG.

To verify the obtained value of shift for all possible input polarization states, an additional measurement of frequency shift was performed using all four polarization states of the PC: -45 , 0 , 90 , and right circular. Maximum and minimum transmission spectra variations were determined by the conventional Mueller technique [10]. The values of the maximum and minimum shifts inferred from these measurements are in line with the results obtained for TM and TE modes, respectively.

In an ideal AWG where the TE and TM modes do not couple, the EO effect in TM mode is expected to be three times stronger than that in TE mode [11]. In our experiments, however, we have found only a small (less than 10%) variation in frequency shifts between the two polarizations. Such behavior might be caused by a combination of EO and electrostriction effects in the presence of optical anisotropy due to a residual stress in the waveguides. A detailed analysis of these contributions to our experiment is yet to be developed. Our preliminary measurements show a significant change in the polarization orientation from input to output of the AWG, indicating a possible averaging of

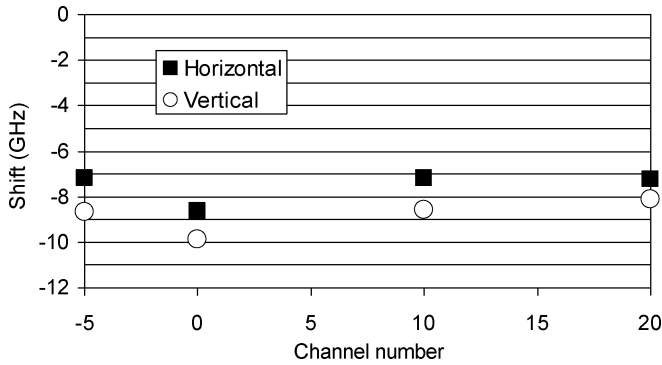


Fig. 4. Magnitude of the frequency shift at 8 kV for different output channels of the AWG for both TE (horizontally polarized) and TM (vertically polarized) input signals.

the EO effect over the polarization states in the waveguide. Note that even without any polarization rotation, it should be possible to achieve polarization-independent tuning by using more complex electrode arrangements.

The experimentally obtained frequency-shift values have satisfactory agreement with values calculated using third-order susceptibility of fused silica. Formula derived for our electrode in the assumption of full polarization averaging is given by

$$\Delta\nu = \frac{2c\chi_{1111}^{(3)}}{\lambda^2 n_0} \frac{D}{M} (1 + \xi) \frac{V^2}{d^2} \quad (1)$$

where $\Delta\nu$ is the central-channel frequency shift, D is the geometrical length increment of waveguide grating, M is the grating order, λ is the central wavelength, c is the speed of light, ξ is the enhancement factor of electrode, $\chi_{1111}^{(3)}$ is the third-order susceptibility of fused silica, n_0 is the refractive index of glass, V is the voltage applied to electrode, and d is the thickness of the silica waveguide structure. A curve representing this formula with no fitting parameters is shown in Fig. 3 by a dashed line. For a given design of EO electrode, the negative sign of frequency shift corresponds to the increase of refractive index with applied voltage. The magnitudes of refractive index change at high voltages (e.g., $\delta n \approx 1 \times 10^{-5}$ at 8 kV) are similar to those obtained in poled-silica EO waveguide structures (e.g., $\delta n \approx 0.65 \times 10^{-5}$ at 5 kV [12]).

In order to estimate the power consumption of EO tuning mechanism, the leak current of electrode was measured. The static power consumption with 8-kV applied voltage is less than 500 μ W and can be further reduced to minimum value of 10 μ W limited by volume electrical resistivity of P_2O_5 - B_2O_3 - SiO_2 -glass system. This nonzero power heats the glass medium and can potentially modify the wavelength shift of the AWG. A rough heat-transfer estimate, however, shows that the corresponding temperature increase is very small (<0.03 °C), yielding less than 0.3-GHz wavelength shift. The low capacitance of electrode (about 50 pF) also allows low power consumption for dynamic control by simple resistive-load controlled circuits. The power consumption analysis generates an additional requirement on the electrooptical

materials for tuning an optical integrated circuit: The ratio between third-order susceptibility $\chi^{(3)}$ and electroconductivity of material σ should be high enough to minimize the power consumption in case of quasi-static stabilization applications or for low-frequency modulation needs. For example, although high-Kerr-coefficient materials such as chalcogenide glasses [13] are good candidates for future reduction of the control voltage, the $\chi^{(3)}/\sigma$ ratio of such materials is not much different from that of fused silica. From this point of view, of particular interest are the silica glass materials with nano-sized particle incorporations [14], where electroconductivity is not changed.

In conclusion, the third-order susceptibility of glass together with a new design of electrooptical electrode is successfully used to control the central frequency of folded AWG in the range of 10 GHz. This frequency tuning has less than 10% of polarization dependence and has a good uniformity across the different channels of AWG. The external power consumption for static 10-GHz tuning was lower than 500 μ W.

Such a phase control mechanism can find applications in low-power-consumption AWG ITU grid adjustment, electrooptical signal processing, and AWG phase error correction.

REFERENCES

- [1] M. Smit and C. Van Dam, "PHASAR-based WDM devices: Principles, design, applications," *IEEE J. Sel. Topics Quantum Electron.*, vol. 2, no. 2, pp. 236–250, Jun. 1996.
- [2] Y. P. Li and C. H. Henry, "Silicon optical bench waveguide technology," in *Optical Fiber Telecommunication IIIA*, I. Kaminow and T. Koch, Eds. New York: Academic, 1997.
- [3] C. R. Doerr, "Planar lightwave devices for WDM," in *Optical Fiber Telecommunication IVA*, I. Kaminow and T. Li, Eds. New York: Academic, 2002, pp. 405–476.
- [4] N. Stelmakh, "Folded design of AWG multiplexer/demultiplexer," presented at the *OSA Annu. Meeting*, Tucson, AZ, Oct. 2003.
- [5] R. Kazarinov and H. Temkin, "Optical Waveguide Transmission Devices," International Patent WO 02/27 372 A2, 2002.
- [6] R. Hellwarth, J. Cherlow, and T.-T. Yang, "Origin and frequency dependence of nonlinear optical susceptibilities of glasses," *Phys. Rev. B*, vol. 11, pp. 964–967, 1975.
- [7] A. Boskovic, S. V. Chernikov, J. R. Taylor, L. Gruner-Nielsen, and O. A. Levring, "Direct continuous-wave measurement of n_2 in various types of telecommunication fiber at 1.55 μ m," *Opt. Lett.*, vol. 21, pp. 1966–1968, 1996.
- [8] R. H. Stolen and C. Lin, "Self-phase-modulation in silica optical fibers," *Phys. Rev. A*, vol. 17, pp. 1448–1453, 1978.
- [9] M. N. Azam and H. Dickinson, "Time lags in the electrical breakdown of glass immersed in water," *Brit. J. Appl. Phys.*, vol. 12, pp. 419–420, 1961.
- [10] D. Derickson, *Fiber Optic Test and Measurement*. Upper Saddle River, NJ: Prentice-Hall, 1998.
- [11] R. W. Boyd, *Nonlinear Optics*, 2nd ed. San Diego, CA: Academic, 2003.
- [12] M. Abe, T. Kitagawa, K. Hattori, A. Himeno, and Y. Ohmori, "Electro-optic switch constructed with a poled silica-based waveguide on a Si substrate," *Electron. Lett.*, vol. 32, pp. 893–894, 1996.
- [13] J. M. Harbold, F. O. Ilday, F. W. Wise, and B. G. Aitken, "Highly nonlinear Ge-As-Se and Ge-As-S-Se glasses for all-optical switching," *IEEE Photon. Technol. Lett.*, vol. 14, no. 6, pp. 822–824, Jun. 2002.
- [14] G. V. Prakash, M. Cazanelli, Z. Gaburro, L. Pavesi, F. Iacona, G. Franzo, and F. Priolo, "Linear and nonlinear optical properties of plasma-enhanced chemical-vapor deposition grown silicon nanocrystals," *J. Modern Opt.*, vol. 49, pp. 719–730, 2002.